SUBCRITICAL WAVE WAKE UNSTEADINESS

A Robbins, G A Thomas, M R Renilson and **G J Macfarlane,** Australian Maritime College, Australia
I W Dand, BMT Isis, UK
(DOI No: 10.3940/rina.ijme.2011.a3.201)

SUMMARY

Vessel wave wake in deep water is well understood, shallow water less so, specifically the effect of restricted water. This operational zone is highly dynamic and non-linear in nature, thus being worthy of closer examination. The paper reviews the primary mechanisms for unsteadiness in wave wake: starting acceleration and soliton generation. A comprehensive set of experiments was conducted using an NPL catamaran hull form to investigate unsteadiness in both wave height and wave angle. The results show that the unsteadiness was primarily due to soliton generation, and that blockage has a significant effect. As a result, additional metrics, aimed at defining shallow water effects in the transcritical region, are proposed.

NOMENCLATURE

A_x	Maximum transverse sectional area (m^2)
b	Tank breadth (m)
B	Maximum demi-hull beam (m)
Fr_l	Length Froude number = $v/\sqrt{(g.L)}$
Fr_h	depth Froude number = $v/\sqrt{(g.h)}$
g	Acceleration due to gravity (m/s)
Hw	Maximum wave height (m)
Hbow	Bow wave height (m)
Hlead	Leading wave height (m)
h	Water depth (m)
k	Blockage = A_x / (b.h)
L	Waterline length (m)
$L/\nabla^{1/3}$	Length - volume ratio
n	wave decay coefficient
s	Demi-hull separation (m)
t	Time (s)
T	Draught (m)
v	Vessel speed (m/s)
x	Longitudinal axis (+ve fwd) (m)
y	Transverse distance from sailing line (m)
Δ	Displacement (kg)
α	Leading wave angle (°)
∇	Volume (m^3)
ρ	Density of water (kg/m^3)

1 INTRODUCTION

As part of an ongoing research program investigating wave wake in shallow water, multiple physical tests have been completed at the Australian Maritime College (AMC) in Launceston, Tasmania utilising the AMC's Model Test Basin (MTB).

The review of the wave height decay results for transcritical wave wake revealed some unexpected findings, which were termed as "unsteadiness". These findings warranted further investigations into (a) starting accelerations and (b) soliton formation. This resulted in an additional test program, on which this paper is based.

The term "unsteadiness" relates to the variation of a vessel's (measured) wave pattern over time. One type of unsteadiness is connected with the way the wave system is initiated within the towing tank or model basin (transient state). The other type is connected to trans-critical effects (steady state) where the critical condition is defined as that existing when depth Froude Number is unity.

Understanding and separating the two categories of unsteadiness is important when analysing experimental and actual vessel wave wake. Without it incorrect conclusions may be drawn from the analysis.

1.1 UNSTEADINESS DUE TO ACCELERATION

As prefaced, one type of unsteadiness is connected with the way the wave system is initiated within the towing tank or model basin. This form of unsteadiness is a function of model starting acceleration and running velocity. It can be described as an oscillatory transient decay phenomenon.

1.1.1 Havelock

In his papers of 1948 and 1949, Havelock [1, 2] described calculations for the wave resistance of a submerged cylinder, in particular the effect on wave resistance when the cylinder is accelerated from rest to a constant velocity.

His analysis determined that the wave resistance oscillated about a steady mean value for a steady state speed, with the oscillations reducing over time. The key question he posed was - "*how long is it before the effect of the starting conditions becomes inappreciable?*" [1].

Havelock determined that the higher the starting acceleration, the lower the oscillation peak value and the quicker the oscillations decay to a steady mean value. In effect the starting acceleration "ramp" has a direct effect on wave pattern resistance and in turn, one can assume, the wave pattern itself.

It must be noted that Havelock's findings related to the calculated wave pattern resistance of a point source – an entirely mathematical postulate. Also these were calculations done for deep, not shallow water. Unlike Havelock, this study is not measuring calculated wave pattern resistance, but using the actual wave elevation measured in model tests.

1.1.2 Wehausen

Wehausen expanded on Havelock's work in his 1964 paper [3], providing more realistic results by utilising thin ship theory rather than point sources. He confirmed Havelock's conclusions that the temporal oscillations in measured resistance were due to the initial acceleration.

Wehausen noted that the form of oscillation decay is asymptotic, which suggests that the oscillations will never entirely decay away. The key question, (as earlier posed by Havelock), is when does this effect become insignificant? In his paper Wehausen stated; "*No matter how quickly the final desired speed is attained by the model, there always remains some question as to how long the influence of the initial accelerations persists and what form this takes*" [3].

Wehausen provided more numerical examples than Havelock and showed too that calculated wave resistance oscillated about the mean as a function of starting acceleration.

Towing tanks had long reported oscillations in resistance measurements, which were primarily thought to come from mechanical resonance within the resistance dynamometers utilised. Experimenters had taken a mean line though the oscillations within the resistance record, and Wehausen's paper confirmed this method as correct.

An interesting observation was made by Wehausen *et al.* [4] during some shallow water experiments. Tests run in the Berkeley towing tank examining the effect of "bottom irregularities" on series 60 models, produced an unexpected outcome. A slowly decaying, periodic response was observed within the wave trace, when the model was driven over the bottom irregularity (a submerged block), or when the model was "hard started" from rest. Wehausen termed this phenomenon as "ringing".

Wehausen noted that variation of the bottom irregularity had little effect on the ringing phenomenon whereas water depth (h), model speed (v), and tank breadth (b), did. Wehausen concluded that this phenomenon is the result of multiple wave reflection from the tank boundaries and has no practical significance for ships. However it should be noted that ships have been known to begin pitching due to bottom irregularities [5].

1.1.3 Calisal

Calisal in his 1977 paper [6] extended the initial acceleration work of Havelock and Wehausen by reviewing the theory with respect to wave pattern measurements. At this time the direct determination of a vessel's wave pattern resistance from wave probes was in vogue.

Calisal determined that: "*the Fourier transform of the wave-height record, provides a possibility of detecting the existence of the initial acceleration effects in the wave system*" [6].

Calisal found that wave pattern resistance deduced from longitudinal cuts was unaffected by initial acceleration (although the wave spectrum might be), whereas that deduced from transverse cuts was. "*One can claim, therefore, that the wave resistance calculations based on fixed probes and longitudinal cuts are not affected by initial acceleration, even though the wave spectrum is*." [6].

1.1.4 Doctors

The previous papers of Havelock, Wehausen and Calisal cover the effects of starting acceleration in deep water, and do so by numerical calculation only. Doctors [7, 8] moved the analysis into shallow water and in particular the trans-critical regime, utilising numerical and experimental results.

Doctors' calculations showed that peak wave height values shift with longitudinal probe location. Furthermore, he concluded that these effects can be largely attributed to the transverse component of the wave system. The question remains how applicable is this finding to the critical condition?

1.2 UNSTEADINESS DUE TO SOLITONS

As prefaced, one type of unsteadiness is due to trans-critical effects: the generation of solitons. This gives rise to another form of unsteadiness which is a function of water depth, displacement, and side boundary; it is a periodic/oscillatory phenomenon even under steady state conditions.

In 1834, John Scott Russell observed the "wave of translation" (*i.e.* soliton) in a Scottish canal. His discovery, later detailed in a paper [9], was not fully exploited until digital computers were able to demonstrate its application in signal transmission. His work is also of significance for vessels operating in shallow water. The behaviour of solitons is the subject of multiple theoretical and physical studies, for example [10, 11, 12].

By definition a soliton is a single wave with no preceeding (or following) trough. In general solitons are cyclical and therefore time dependant. The time step cycle of a soliton can be approximately described diagrammatically for a vessel travelling at constant speed in Figure 1.

At the critical depth Froude number, the vessel's leading wave will grow from a minimum value, (time = 0% - point A), to a maximum at its fully developed state (time = 100% - Point D). The leading wave (soliton) will then shed forward from the vessel (Point E), and a new leading wave will be formed, steadily growing once again to a maximum value. While the model speed remains constant, there are associated changes in resistance, sinkage and trim which follow this wave growth cycle. This oscillatory behaviour will continue as long as time (*i.e.* facility length) permits.

Ertekin *et al*. note that an important property of a soliton is that its speed is supercritical [13], so once the wave is generated and then shed from a model, it will travel along the tank, leaving the model behind, for the cycle to restart afresh.

It follows that for a vessel travelling at, or around the critical depth Froude number, (where soliton growth is present), any wave wake measurement made will be time dependant. Figure 2 is a conceptual diagram of this time dependency. The wave elevation at "A" is significantly different to that at "E", where a full soliton has been formed and shed. Specific tests in a larger facility would be required to fully populate such a diagram, and determine its actual shape with respect to magnitude and form.

1.3 RESTRICTED WATER

The flow around a vessel can be restricted vertically (*i.e.* depth), or laterally (*i.e.* width), or both vertically and laterally giving rise to the effect known as blockage [14].

To quote Saunders, [15], "*A body of water is considered to be shallow when the boundaries are close enough to the ship to affect its resistance, speed, attitude, manoeuvring, and other performance characteristics as compared to its corresponding behaviour in a body of water of unlimited depth"*. In general this is due to the increased potential flow around the hull caused by its proximity to the bottom [16].

The most common water restriction is depth, which is generically termed as "shallow water". In general terms the depth Froude number helps define whether the speed is sub-critical, critical or super-critical, while depth-length (h/L) or depth-draught (h/T) ratio may define the "shallowness" of the water in an absolute sense.

It is not common to have the flow around a vessel restricted laterally only. More commonly both lateral and vertical flow restriction occurs, such as when a vessel travels in a canal or channel and experiences blockage. An experimental test facility, either towing tank or model basin, will restrict the flow around a model.

Blockage can be described numerically in terms of the blockage coefficient (k), which is a function of vessel cross sectional area (A_x), tank width (b), water depth (h) in the form $k = A_x / (b.h)$.

The effect of blockage on vessel speed loss, (or increased resistance), has been well covered in the literature: Schlichting [16], Lackenby [17], Baker [18] and Landweber [19]. However the blockage effect on vessel wave wake has received less attention.

One core concern is that a towing tank does not have the ability to vary breadth in order to explore the effect of lateral restriction, while the broader model basin does not necessarily have the length required to see a full soliton cycle.

1.3.1 Soliton Generation

Lamb [20] has demonstrated that solitons occur at the critical depth Froude number, however it is unclear whether ship generated solitons can occur at higher, (or lower), speeds than at the critical depth Froude number. Remembering that depth Froude number is a simplistic, depth specific measure, based on a single travelling pressure source, it is known [21, 22], that soliton amplitude and period are functions of water depth (h), tank width (b), and depth/draught ratio (h/T), (*i.e.* blockage).

Ertekin [13] conducted experiments to investigate the effect of blockage co-efficient variation on soliton generation. He observed solitons occurring over a range of depth Froude numbers from Fr_h 0.9 to Fr_h 1.2, not just at the critical value. It was further reported that, for both measured and calculated experiments, the resistance oscillated about a mean value, with a period equal to that of soliton generation.

Some of his key findings were that: (a) for an increase in tank width - soliton wave amplitude decreases; (b) for an increase in tank width - soliton period increases; (c) the soliton amplitude curve characteristics are almost identical for the same blockage value, despite significant change in water depth.

Lyakhovitsky [23], in his numerical investigations of ships travelling in a canal, presented the idea that rather than being a single fixed point at $Fr_h = 1$, there are separate boundaries between sub-critical, critical and super-critical flow states. Furthermore, that these critical boundaries diverge with increasing blockage.

Figure 3 is a direct reproduction from Lyakhovitsky's book, and describes the sub-critical, critical and super-critical boundaries. Said boundaries are obtained from his novel one-dimensional hydraulic theory, which while not theoretically rigorous, are in accord with the present results.

The depth Froude number used in combination with the blockage coefficient may therefore provide a better understanding of the flow regime a vessel is travelling in, according to its physical surroundings.

1.4 CURRENT INVESTIGATION

As aforementioned, the Authors' previous investigations into shallow water wave wake decay highlighted some unexpected results related to unsteadiness, [24]. From the theory above it is clear that said previous experiments may have experienced shallow water unsteadiness, probably related to blockage and depth Froude number. Therefore an additional test program was proposed to investigate the possible causes of this unsteadiness.

The key questions are:

a) Has the wave pattern settled to a steady state by the primary measurement location?
b) What is the limit of the unsteadiness?
c) How does this affect the experimental results?

2 PHYSICAL TESTING PROGRAM

2.1 HULL FORM

The model was of a catamaran configuration and the hull form utilised was a variant of the National Physical Laboratory (NPL) series. The parent NPL hull was originally developed by Bailey [25] and utilised to create a design tool for high speed vessels. Molland and Lee [26] further modified this form for their investigations into the effect of prismatic coefficient on catamaran and monohull resistance. Their parent hull form, 5b, is referred to here as the NPL+ hull form. The NPL+ parameters are shown in Table 1, and the body plan is shown in Figure 4.

Parameter	**NPL+** (Heavy / Light)
L (m)	2.50 / 2.48
B (m)	0.23 / 0.22
T (m)	0.11 / 0.10
Δ (kg)	51.3 / 40.0
s/L	0.4 / 0.4
Trim	0° / 0°
Ax	0.0340 / 0.028

Table 1 – NPL+ Parameters

2.2 TEST PROGRAM

Eight conditions were tested, (two displacements and four water depths), each for a range of speeds. Over 120 runs were completed; with the outline test program shown in Table 2.

For this part of the work, (i.e. focussing on wave unsteadiness), only those results up to the critical Froude depth number were examined. The Authors' previous paper [24] covered the full trans-critical range, and it is the intention to extend this work in the future.

Parameter	Range
v (m/s)	0.59 – 2.80
Fr_h	0.30 – 1.00
Fr_L	0.17 – 0.57
h (m)	0.20 – 0.80
h/L	0.08 – 0.32

Table 2 - Test Hull Form Parameters

2.3 MODEL BASIN

The AMC MTB is 35 m long, 12 m wide and has a water depth range of zero to 1.0 m. It is fitted with an electric winch system capable of towing models up to a maximum speed of approximately 3.75 m/s and a multi-segment wave maker. The bottom of the basin is flat to a tolerance of ±10 mm, providing the ability to conduct accurate experiments in very shallow water depths. The combination of large width (compared to a towing tank), solid flat bottom, variable water depth, model towing winch and wave generation capability makes this facility very versatile. For these tests, wave damping materials were added along the tank walls to minimise wave reflections.

2.4 PROBE ARRANGEMENT

An array of wave probes was utilised to ensure detailed and accurate measurement of the generated wave patterns. Seventeen 300mm long wave probes were mounted on four aluminium beams, the final probe arrangement being shown in Figure 5. The time taken to conduct each calibration became a significant factor due to the number of probes and water depths changes.

The main transverse array measured wave height, decay (as a function of transverse distance from the sailing line), and leading wave angle, (probes 1, 2, 3, 4, 5, 6, 7, 8 and 9). The secondary transverse arrays measured leading wave angle only, (probes 12 + 13 and probes 10 + 11). The longitudinal array measured wave "growth", (probes 15, 16, 12, 17, 9, 18 and 9).

The digital data acquisition equipment recorded each run for approximately 35 seconds at a sample rate of 200 Hz.

3 EXPERIMENTAL RESULTS

3.1 LEADING WAVE METRIC

As covered in the Authors' previous work on trans-critical wave wake [24], the use of the maximum wave height (Hw) as the primary measure across the trans-critical range was not recommended.

Wave cut analysis of the measured data showed significant superposition of competing wave systems. In addition the position of the maximum wave height changed unexpectedly across the transverse probe array, providing erroneous results.

Instead the bow wave's height (Hbow) was utilised as a suitable metric because it is easily identifiable across the trans-critical range and still provides similar decay characteristics. It has since been recognised that the use of the term "bow wave", in the far field, may not be entirely accurate. Therefore, a more suitable alternative, "leading wave" (Hlead) been utilised as the primary wave height measure within this work.

3.2 ERROR ANALYSIS

Error analysis, (uncertainty analysis), is important in establishing a baseline of confidence for any data set. For this work it has been not only utilised to establish accuracy, but also in determining if wave growth is occurring. The standard deviation method was utilised to establish a baseline error for these tests, (where standard error = standard deviation / √ number of observations).

For this, repeat runs were made at a fixed depth across the sub-critical range, and also at a fixed depth Froude number across multiple water depths. Hlead was the metric utilised.

Repeat runs were completed across the subcritical range, (Fr_h = 0.5 - 1.0), at a fixed water depth of 200mm. Figure 6 is a plot of the Hlead standard deviation, as a function of Fr_h, for a number of different transverse offsets. From this plot the maximum standard deviation across all runs is seen to be 0.25.

Repeat runs were completed at the four water depths (h = 200, 400, 600, 800 mm) at a fixed Fr_h of 0.5. Figure 7 is a plot of the Hlead standard deviation for each water depth, and a number of different transverse offsets. From this plot the maximum standard deviation across all runs is again 0.25.

For constant Fr_h and constant water depth – across all transverse probes – the error appears to be relatively constant with a maximum value of 0.25. This is in keeping with the Authors' previous work [24]. It was therefore assumed that any standard deviation value above 0.25 would be an indicator of growth or unsteadiness.

3.3 WAVE GROWTH

To determine if a vessel's wave wake is unsteady the main longitudinal array of wave probes was utilised, refer Figure 5. A comparison of the resultant measured wave heights at various longitudinal locations revealed if growth was occurring.

The results are as plotted in Figure 8 and it is clear that there is significant leading wave growth occurring around the critical Fr_h number, whereas at low Fr_h numbers there is no growth detected.

Standard deviation shows how much variation there is from the average or mean, but does not indicate growth (positive value) or decay (negative value). It was decided that a more descriptive measure was required, which would indicate if growth or decay (or neither) was occurring.

Accordingly, the dy/dx value (slope) of a line fitted through the (averaged) points of longitudinal Hlead was utilised. The dy/dx baseline error has been determined to be 0.1. The results are in Figure 9, which displays very similar results as for Figure 8.

The lowest water depth (200mm) exhibits the highest level of growth, (both standard deviation and slope), with growth detected from Fr_h 0.80. The highest water depth (800mm) exhibits the lowest level of growth, (both standard deviation and slope), with growth detected at Fr_h 0.65.

The lower displacement (40kg) results exhibit marginally lower levels of growth than those for the heavier displacement (51kg), albeit at a higher Fr_h value. Note that T and k are both greater for the heavier displacement, with h/T being smaller.

From these results it can be concluded that wave growth is occurring within the experiments, and occurs at speeds as low as Fr_h = 0.7. Water depth has a significant effect on wave growth with respect to its level and inception point, while displacement has only a secondary effect. These findings have been summarised in Table 4.

3.4 LEADING WAVE ANGLE

One possible cause of the unexpected results highlighted in the previous work [24] on transcritical wave wake decay, was that the wave system was not fully developed. To investigate this claim, the leading wave angle was measured at multiple positions longitudinally utilising the transverse wave probe arrays.

Referencing Figure 5, the leading wave angle was measured using probes 1 + 9 on the main transverse array, probes 12 + 13, and probes 10 + 11 on the secondary transverse arrays. Each array was spaced longitudinally at 2m, (0.8L).

The leading wave angle was measured from Fr_h 0.3 – 1.0, at 200mm, 400mm, 600mm, and 800mm water depths. The data was processed to provide the leading wave angle from each run at each array.
The results are in keeping with the Authors' previous leading wave angle findings [24], namely that the peak value occurs around $Fr_h = 0.9$, (not at $Fr_h = 1.0$) and the wave angle remains at the "deep water" value of 19°28' for $Fr_h < 0.7$. These findings have also been summarised in Table 4.

Figure 10 shows a plot of leading wave angle as a function of depth Froude number, measured at the three arrays, for h = 800mm. It is clear that for $Fr_h < 0.7$ there is little or no variation in measured angle between the arrays. This is a trend which continued for the other three water depths tested.

For $Fr_h > 0.7$ there is a slight divergence in the measured angles, although this is within the error margin. Similar trends are found for the other depth conditions, although not as pronounced. The results indicate that the leading wave angle has settled, across the depth Froude number range, and all water depths tested.

3.5 SOLITON GENERATION

As mentioned before, due to the blockage characteristics of the model basin, and taking into account previous experimental studies [13, 21, 22, 27], it was probable that any soliton generated would be of low amplitude and long period.

It was decided that soliton identification would best be achieved by inspection of longitudinal wave cuts and further supported with enhanced photographs.

In addition to the physical wave probe measurements, many photographs were taken of the experiments. To enhance the standard photo a series of white rope lights were fixed to the basin's ceiling. The lights' reflections on the water's surface made identification of the resultant wave pattern clearer. While not a true measurement, these images provided an excellent identification aid, see Figure 11.

The longitudinal cut utilised for inspection was taken from Probe 17 on the main transverse array. This probe was the most outboard and forward of the probes available, being clear of possible local wave effects, and allowing maximum wave development.

From observations of the enhanced photographs and longitudinal wave cuts, a summary table, (Table 4), has been generated. This table highlights when a soliton has been observed in the photograph and in the wave cut. The wave cut for the observed soliton has been reproduced in Figure 12.

From a closer review of the wave cuts, for example Figure 13, (*i.e.* run 92, $Fr_h = 0.9$, h = 200mm), it can be seen that they exhibit a similar wave profile to that of Figure 12, albeit under-developed. Furthermore these wave cuts, showing an under-developed soliton form, closely match those runs also exhibiting unsteadiness, (ref Figure 8). This suggests that there is the possible onset of a soliton. However due to limited run time, (*i.e.* limited facility length), it has not developed sufficiently to be identified correctly as a soliton. This has been noted in Table 4 as "Onset".

While only one soliton was clearly observed, it is possible that given more run time, solitons would also have been observed at the deeper water depths of h = 400, 600, and 800mm, (Ref Figure 14, Figure 15 and Figure 16). Accordingly these runs have been noted in Table 4 as "None". Furthermore it is proposed that for some near-critical runs at shallower water depths, given more run time, solitons would have developed.

Figure 17 is a plot of results from longitudinal probes for $Fr_h = 1.0$ and h = 200mm. This figure clearly shows the development of the soliton. A review of probe 17 for $Fr_h = 0.9$ shows similar wave form as those appearing at 14 for $Fr_h = 1.0$. This would suggest that, given more run time, fully developed solitons could occur at the lower depth Froude numbers.

A further review of Figure 12 shows a smaller peak forming directly behind the soliton, which suggests that a second soliton may be forming. This is in keeping with the oscillatory nature of solitons, as seen in other experimental works [13, 22].

Dand *et. al.* [22], in their work on catamarans operating in shallow water, reported; "*Rather than a single wave, the disturbance ahead of the model consisted of a number of solitary waves with the process of creation occurring continuously along the tank. This suggests that the assumption that such waves are created simply by the starting transients of the models at the beginning of a run is incorrect.*" Therefore the presence of a second soliton would indicate that the observed unsteadiness is not caused by starting accelerations.

Figure 18 is a composite of Figure 3, (Lyakhovitsky plot), and Table 4, (results summary table). The NPL+ hull form tested in the AMC MTB, has be added to the original diagram. The blockage for each of the four water depths investigated are indicated in this figure.

There is some agreement with the numerical predictions, although greater concurrence may have been achieved had model run time been longer, (enabling full soliton development near the critical Fr_h). Additionally an increased number of runs, at finer Fr_h resolution, may have revealed a clearer definition of the behaviour.

3.6 DISCUSSION

3.6.1 Unsteadiness

As already discussed, unsteadiness in the wave pattern can be accounted for by either starting accelerations, or from the generation of solitons near the critical depth Froude number. Starting acceleration unsteadiness can be discounted primarily as there was no evidence of it at low speeds. Secondary soliton generation at higher speeds confirms this finding.

However despite the runs at Fr_h 0.7 and 0.8 showing unsteadiness, (Figure 9), and shallow water leading wave angle, (Figure 10), no solitons were observed within the longitudinal wave cuts. This finding concurs with previous shallow water testing at the AMC MTB, where no solitons were observed at such low Fr_h.

The question remains what is causing the recorded unsteadiness? It is possible that these sub-critical, shallow water, leading waves are still developing, and a longer model run time may show them develop to a steady state, (but not into solitons). It is equally possible that these runs are close to the transitional boundary between the sub-critical and critical zone.

While only one soliton was actually recorded, (at the shallowest water depth and at the critical number), the onset of solitons was observed at the near critical Fr_h of 0.9, (Figure 13). This suggests that the Lyakhovitsky theorem [23], (of blockage dependant boundaries between sub-critical, critical and super-critical flow states), is correct.

3.6.2 Operational Zones

For this work the definable wash zones are: (1) Sub-Critical Deep, (2) Sub-Critical Shallow and (3) Critical Shallow. The metrics used to define each zone are; (a) Leading Wave Angle, (b) Steadiness and (c) Soliton. The criteria for each zone, (i.e. proposed shallow water metrics), are shown in Table 3.

The metrics given in Table 3 relate to those parameters which indicate whether or not the vessel is experiencing different physical conditions as a result of the proximity of the bottom. For example, if the leading wave angle is different to that in deep water, then this is an indicator that the vessel is influenced by the bottom in this case. Equally, if the wave height is varying with time (or distance along the x axis) then this indicates that physically the vessel is in a regime other than 'deep' water.

Furthermore, said metrics are used by the authors to determine whether the vessel, at the given speed, water depth, draught, and blockage is influenced by the presence of the bottom. Parameters commonly used such as H/T and Frh do not do this, but are simply non-dimensional values which indicate how close the vessel is to the bottom, or what speed it is travelling at. On their own they are *not* measures of whether a particular vessel in a particular condition is influenced by the presence of the bottom, or not.

Table 4 summarises the test results, utilising the aforementioned metrics and resultant zones, for each Fr_h and water depth. These outcomes have also been included into Figure 18.

3.6.3 Critical Wave Wake Measurement

From the test results, soliton generation has been recorded within the wave cuts and observed from photographs. However as the basin has a finite length, it was not possible to record a complete soliton cycle. It follows that the wave patterns measured around the critical number are "snapshots" of this time dependant phenomenon. Furthermore any measurement needs to be referenced by a "time stamp" of where it occurs within the cycle, reference Figure 2.

There exist high and low Fr_h limits outside which wave growth can be considered as negligible, and the wave pattern could be considered as steady. These zones could be known as "shallow water steady" and "deep water steady". The zone inside these limits could be known as "shallow water unsteady" zone, as shown in Figure 3 as the critical zone.

3.6.4 Effect on Wave Decay

In the Authors' previous work [24], covering the trans-critical zone (Fr_h 0.3 - 2.5), the results of leading wave decay were presented.

The results showed a large variation in the decay coefficient (n), specifically around the critical number. It is now clear that these measurements were most likely unsteady and time dependant. In turn the decay coefficient presented was affected and it is worth reiterating that any measurements taken within this unsteady zone are a snap shot within the cycle, and should be qualified by a time stamp.

3.6.5 Variation of Displacement

While displacement has a significant effect on wave height [24], it appears to have an insignificant effect on wave growth, (*i.e.* unsteadiness). This may because of the relatively low blockage (k = 0.0035) at which the effects of displacement were tested.

It has been suggested that blockage seems to be the key factor in unsteadiness [21]. It is probable that at higher blockages, displacement will have an increasingly significant effect. Further testing would be required to determine this.

3.6.6 Facility Limitation

It is known that soliton generation is a function of physical parameters such as tank width, water depth, model speed, model acceleration, model displacement and tank length. Accordingly wave measurements should be considered specific to the facility and the models tested within it. The higher the blockage value the more specific they become.

These tests have shown that boundaries exist for unsteadiness within the AMC MTB. These boundaries are functions of blockage water depth and model speed. It is probable that model hull form and hull arrangement (*i.e.* monohull / catamaran), also have an effect on said boundaries. It is recommended that more tests be undertaken to develop a comprehensive understanding of shallow water wave growth within the AMC MTB. This would require large permutations of water depth, facility width, model speed, model hull form, model draught, model arrangement. Whittaker [28] in his SWIM work realised similar limitations of working in a relatively short model test basin.

Determining the complete global understanding of shallow water wave growth would require significant work. As such near critical unsteadiness, (*i.e.* wave growth), should be considered a standalone topic.

4 CONCLUDING REMARKS

The Authors' previous physical testing, investigating shallow water wave wake decay, highlighted some unexpected findings. In turn, further physical tests into the effect of starting accelerations and soliton formation were completed.

These tests determined that, as the critical number is approached, it is most likely that the formation of solitons, not starting accelerations, which are the cause of the reported unsteadiness. For the lower Fr_h runs which exhibited unsteadiness, it is most likely that insufficient run time is highlighting an under developed leading wave.

Furthermore, the blockage of the test facility is a key consideration in sub-critical wave wake, having a potentially significant effect on the measured results. It is recommended that the depth Froude number and blockage should be utilised as a combined measure of shallow water unsteadiness.

It is noted that due to the time dependant nature of near critical unsteadiness, wave wake measurements should be referenced with a time stamp. Also, that more research is required to understand this problem fully.

The wider (*i.e.* full scale) implications of these model test findings are potentially significant. All previous wave wake measurements, taken around the critical Fr_h, will be time dependant (*i.e.* unsteady). This is especially true in high blockage environments such as rivers or canals. A new metric may be required to measure this unsteadiness adequately.

5 ACKNOWLEDGEMENTS

The authors would like to acknowledge the AMC facility staff for their considerable work in setting up the AMC MTB for the experimental program, particularly with the large wave probe array.

6 REFERENCES

1. Havelock, T. H. “The Wave Resistance of a Cylinder Started from Rest” Quarterly Journal of Mechanics and Applied Mathematics, Vol II, Pt 3, 1949. (Also Collected Works page 536-544).

2. Havelock, T. H. “The Resistance of a Submerged Cylinder in Accelerated Motion” Quarterly Journal of Mechanics and Applied Mathematics, Vol II, Pt 4, 1949. (Also Collected Works page 545-553).

3. Wehausen, J.V. “Effect of Initial Acceleration upon the Wave Resistance of Ship Models” Journal of Ship Research, January 1964, p38-50.

4. Sibul, O.J., Webster, W. C., & Wehausen, J. V. “A Phenomenon Observed in Transient Testing” Schiffstechnik, Vol. 26, pages 179 -200, 1979.

5. Renilson, M.R. and Hatch, T., ‘A Preliminary Investigation into Squat Over an Undulating Bottom’, The Naval Architect, February 1998, pp. 36-37.

6. Calisal, S. “Effect of Initial Acceleration on Ship Wave Pattern and Wake Survey Methods”, Journal of Ship Research, December 1977, p239-247.

7. Doctors, L. J. “The Unsteady Growth of Ship Waves in a Towing Tank” Journal of Ship Research, Volume 54, Number 2, June 2010, pp. 120-132.

8. Doctors, L.J ., Day, A.H., and Clelland D., “Unsteady Effects during Resistance Tests on a Ship Model in a Towing Tank”, Journal of Ship Research, Vol 14, No 3, 2009.

9. Scott Russell, J.: "Report on Waves": Report of the fourteenth meeting of the British Association for the Advancement of Science, York, September 1844.

10. Mei CC. “Radiation of solitons by slender bodies advancing in a shallow channel”. J Fluid Mech 1986;162M43:53-67.

11. Mei CC. “Flow around a thin body moving in shallow water”. Journal Fluid Mechanics 1976;77(4):737-751.

12. Ertekin, R.C.,Webster, W.C. and Wehausen, J.V. (1986), "Waves Caused by a Moving Disturbance in a Shallow Channel of Finite Width", J. Fluid Mechanics, Vol. 169, pp.275-292.

13. Ertekin, R.C., Webster, W.C., and Wehausen, J.V., University of California, Berkley, USA. “Ship Generated Solitons”" Proc. 15th Symposium of Naval Hydrodynamics, Hamburg, Germany, 1984.

14. BSRA: “Hydrodynamics” British Ship Design Manual, Issue 2, August 1981.

15. Saunders, H. E., “Hydrodynamics in Ship Design”, 3-volume set, The Society of Naval Architects and Marine Engineers (SNAME), 1957.

16. Schlichtling, O. “Ship Resistance in Water of Limited Depth – Resistance of Sea-going Vessels in Shallow Water” Jahrbuch der STG, Vol 35 1934.

17. Lackenby, H. “The Effect of Shallow Water on Ship Speed”. Shipbuilder and Marine Engineer Vol 70 (1963).

18. Baker G.S., “Ship Form, Resistance and Screw Propulsion”, New York: D. Van Nostrand Co., 245p, 1915.

19. Landweber, L. “Tests of a model in Restricted Channels” EMB Report 460, May 1939

20. Lamb, H. “Hydrodynamics”. Cambridge University Press, Cambridge, UK, 1932.

21. Whittaker, T.J.T., Doyle, R., Elsaesser, B., ‘An experimental investigation of the physical characteristics of fast ferry wash’, Proc. 2. Int. Conf. on High-Performance Marine Vehicles HIPER, HSVA, Hamburg, May. 2001.

22. Dand, I. W., Dinham-Peren, T.A. and King, L. “Hydrodynamic Aspects of a Fast Catamaran Operating in Shallow Water”. Proceedings of RINA International Conference on the Hydrodynamics of High Speed Craft, London, 1999.

23. Lyakhovitsky, A., “Shallow Water and Supercritical Ships” Backbone Publishing, ISBN 9780974201955, 2007.

24. Robbins, A. W., Thomas, G., Renilson, M., Macfarlane, G., Dand, I., “Vessel Tran-scritical Wave Wake, Divergent Wave Angle and Decay” Vol 151, IJME Royal Institution of Naval Architects, London, 2008

25. Bailey, D. “The NPL High Speed Round Bilge Series.” Maritime Technology Monograph No.4, RINA, 1976.

26. Molland, A. F. and Lee, A. R. “An investigation into the effect of prismatic coefficient on catamaran resistance”. Royal Institution of Naval Architects, London, 1997.

27. Dand, I. W. “The Effect of Water Depth on the Performance of High Speed Craft” High Performance Yacht Design Conference, Auckland, 2002

28. Doyle, R., Whittaker, T.J.T., Elsaesser, B., ‘A study of fast ferry wash in shallow water’, Proc. Fast 2001, RINA, Southampton, Sept. 2001, 14 pages.

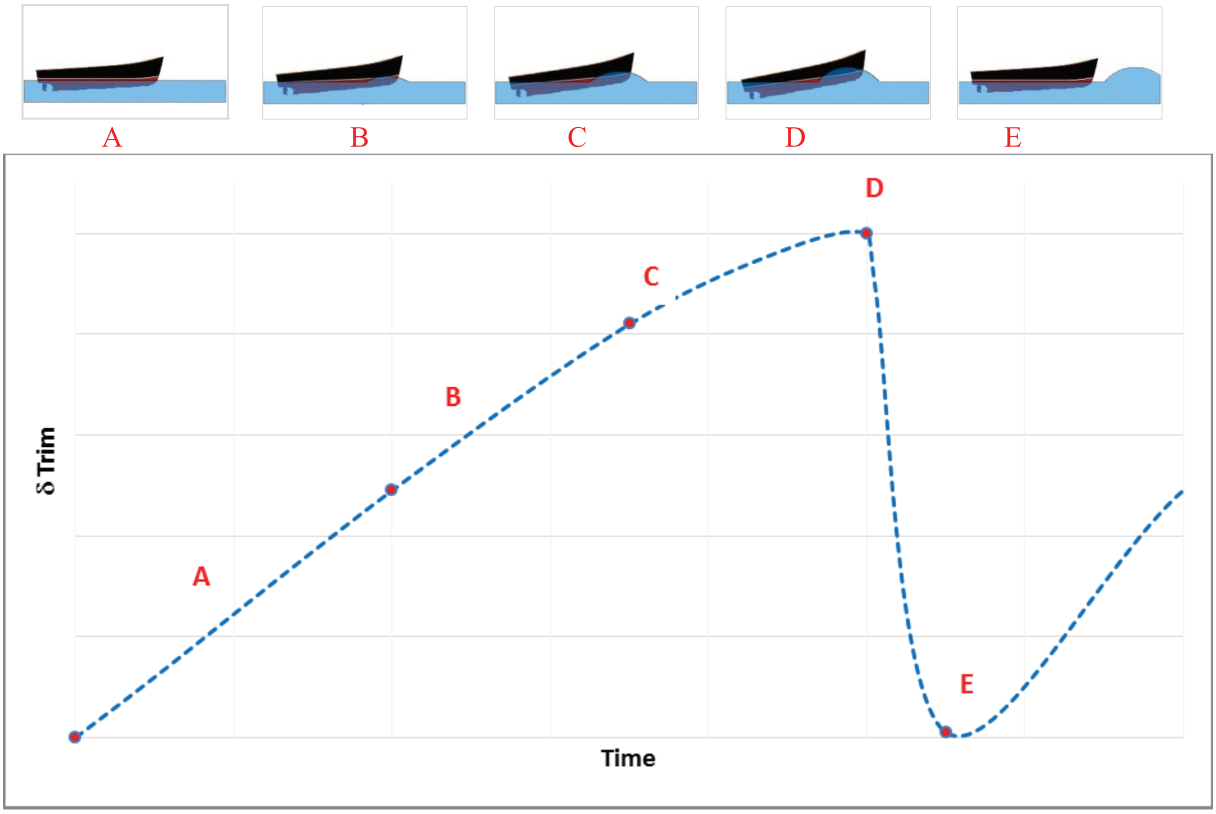

Figure 1 – Illustration of Soliton Life Cycle

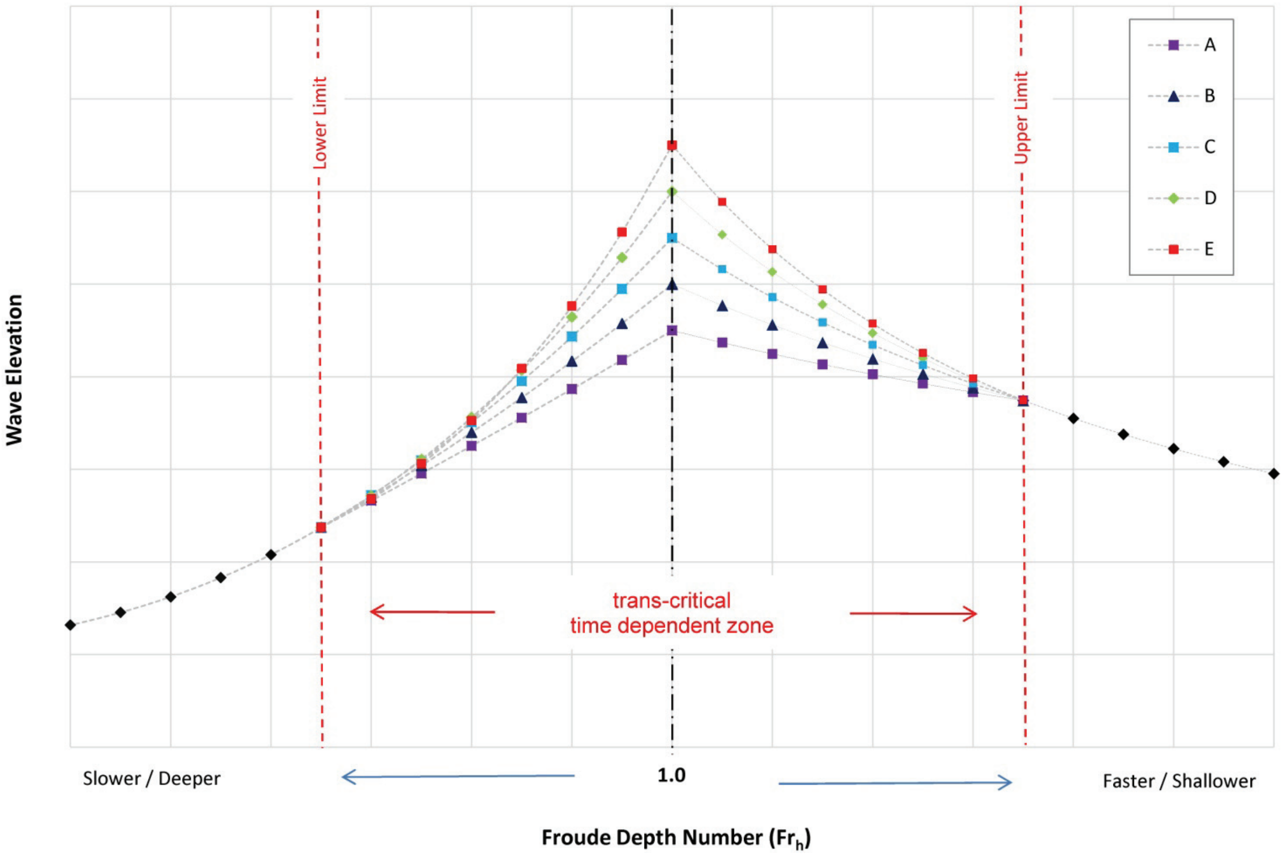

Figure 2 – Conceptual Diagram of Time Dependant Wave Height

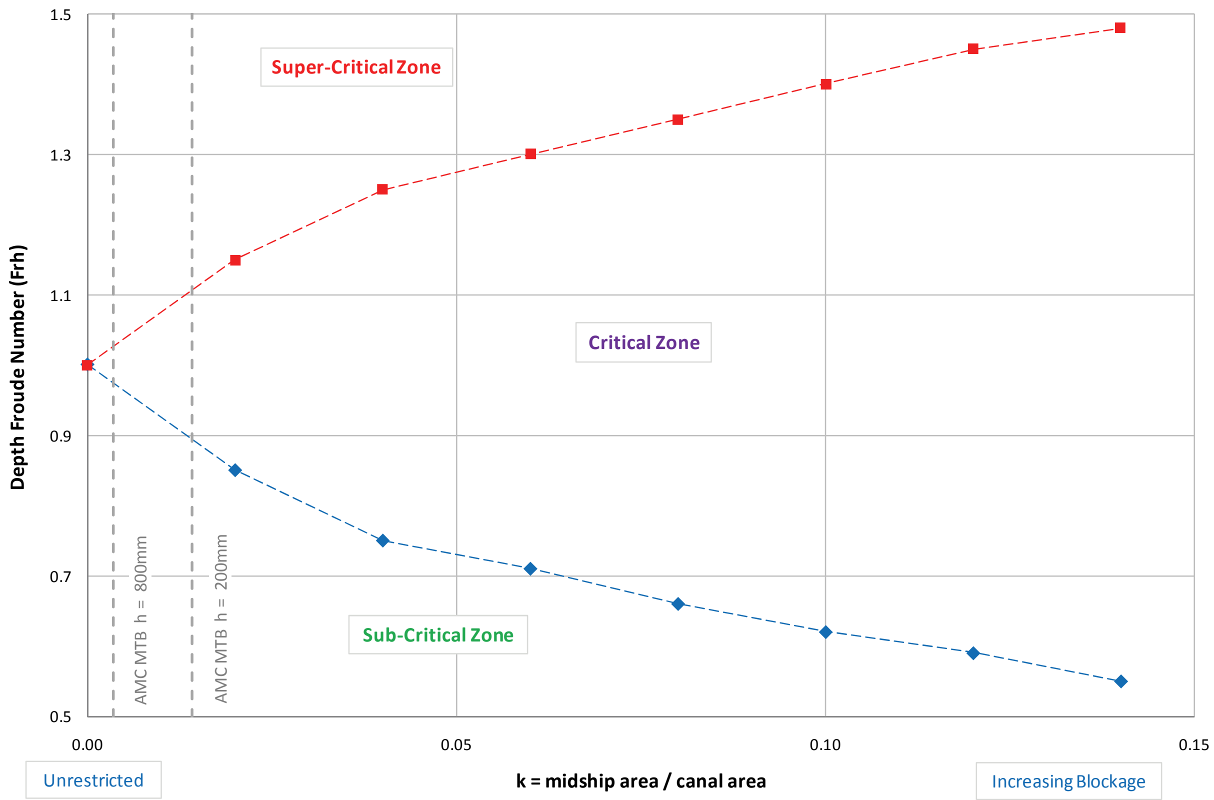

Figure 3 – Critical Boundaries - (adapted from Ref [23])

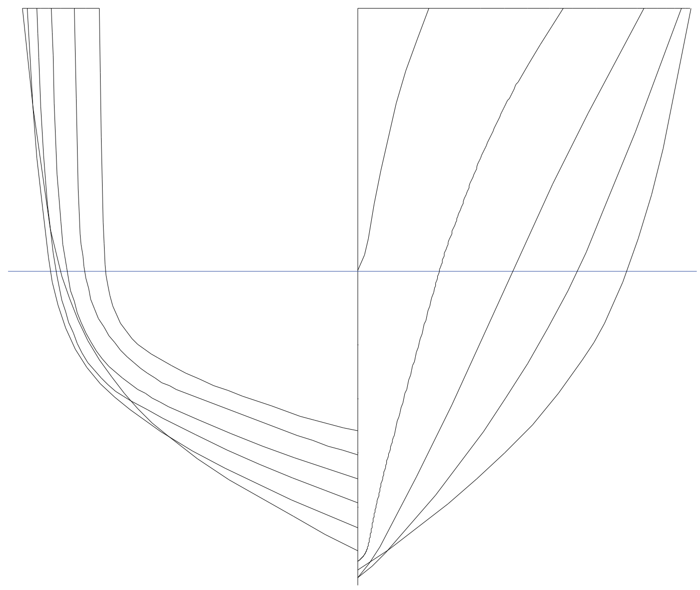

Figure 4- NPL+ Hull Form

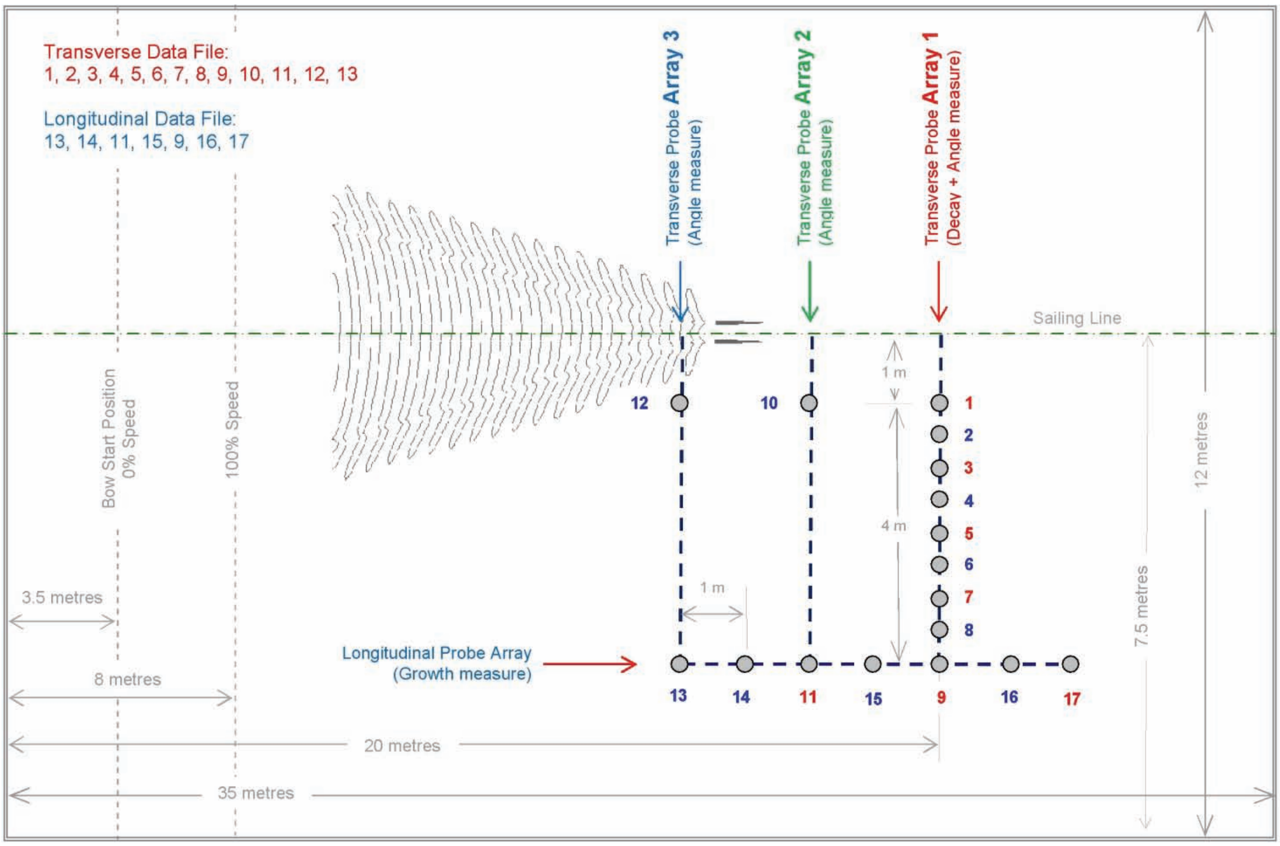

Figure 5 – Probe Arrangement.

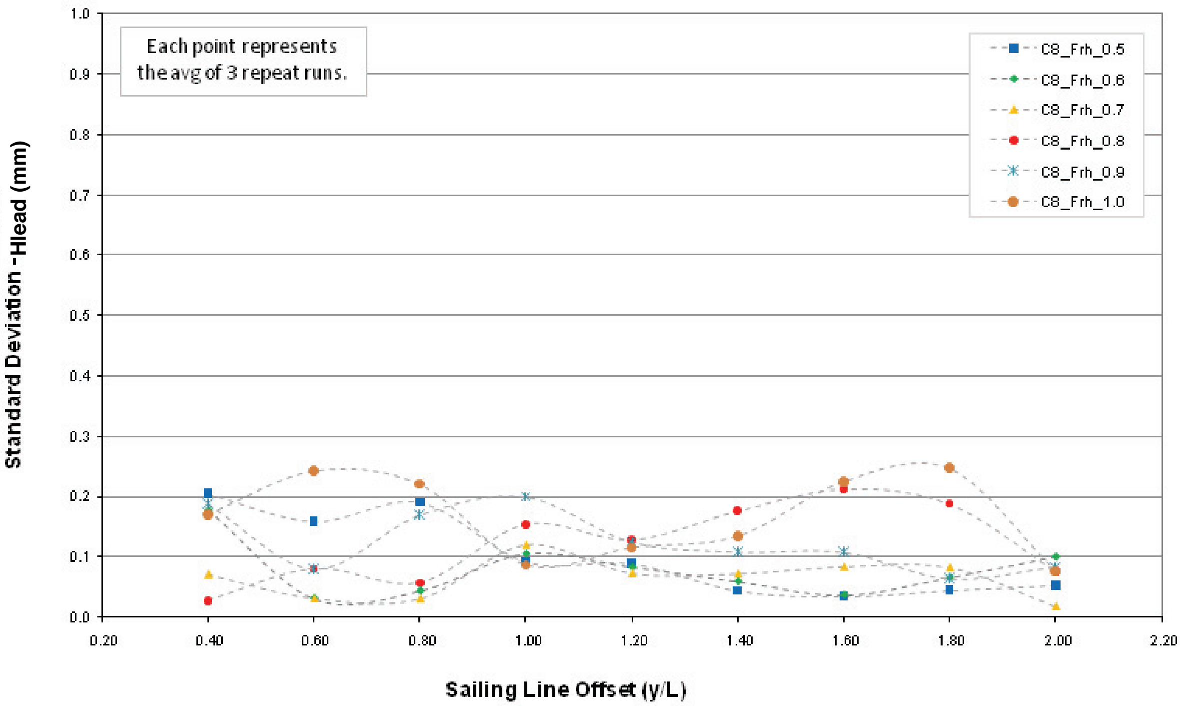

Figure 6 – Error for Fixed Depth (200mm)

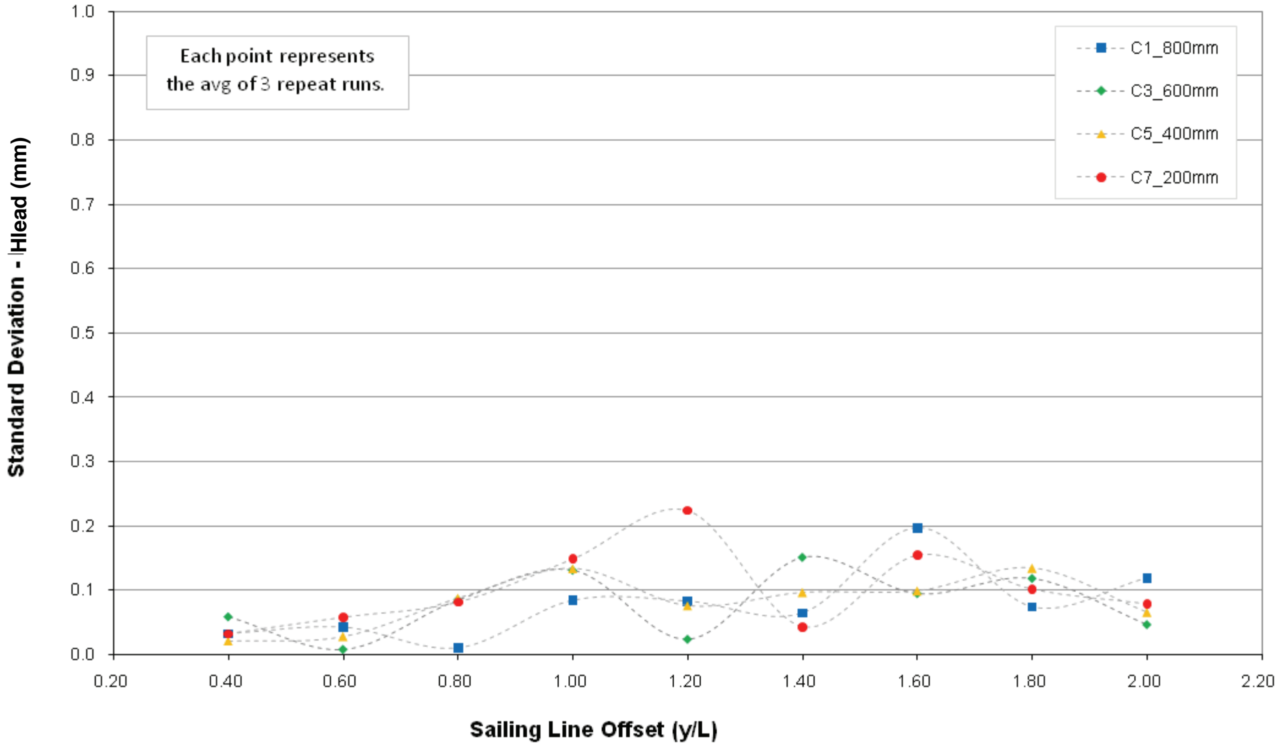

Figure 7 – Error for Fixed Fr_h 0.5

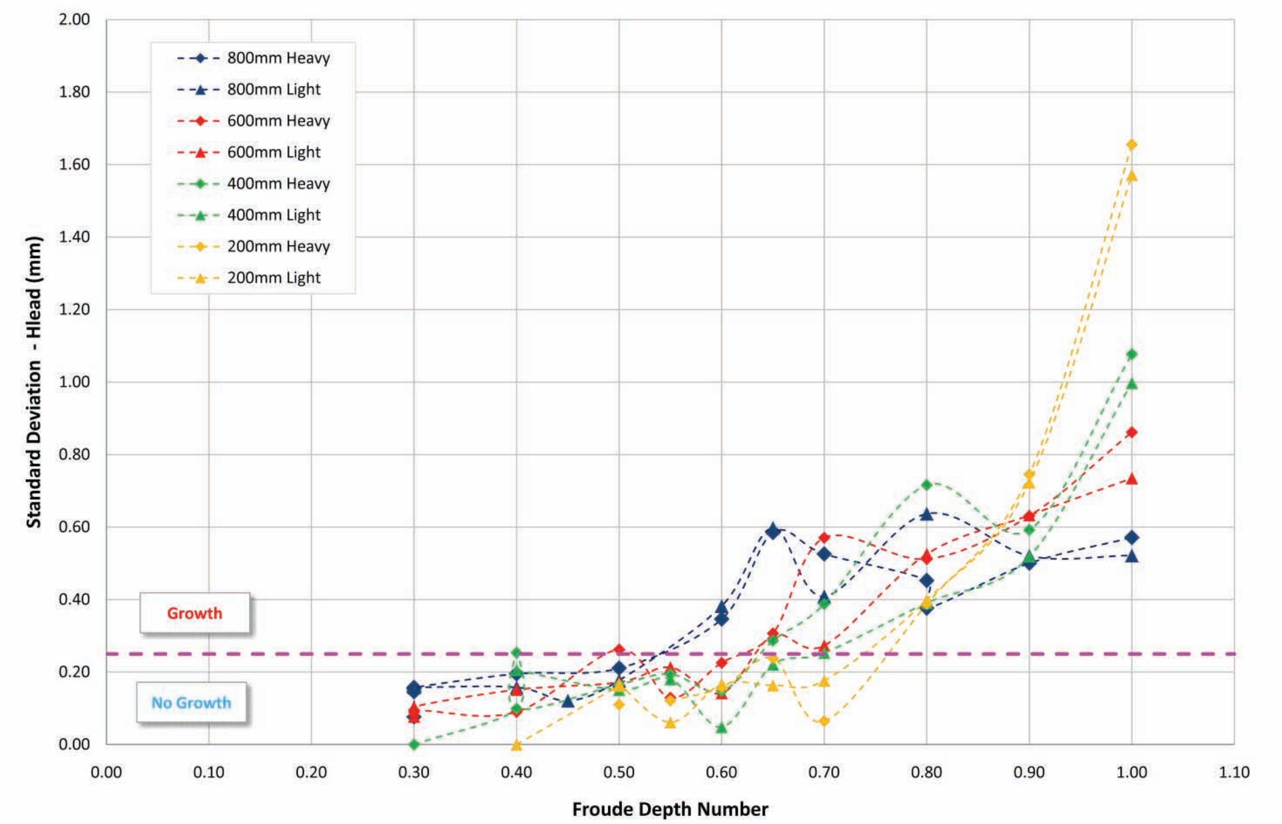

Figure 8 – Leading Wave Height Standard Deviation

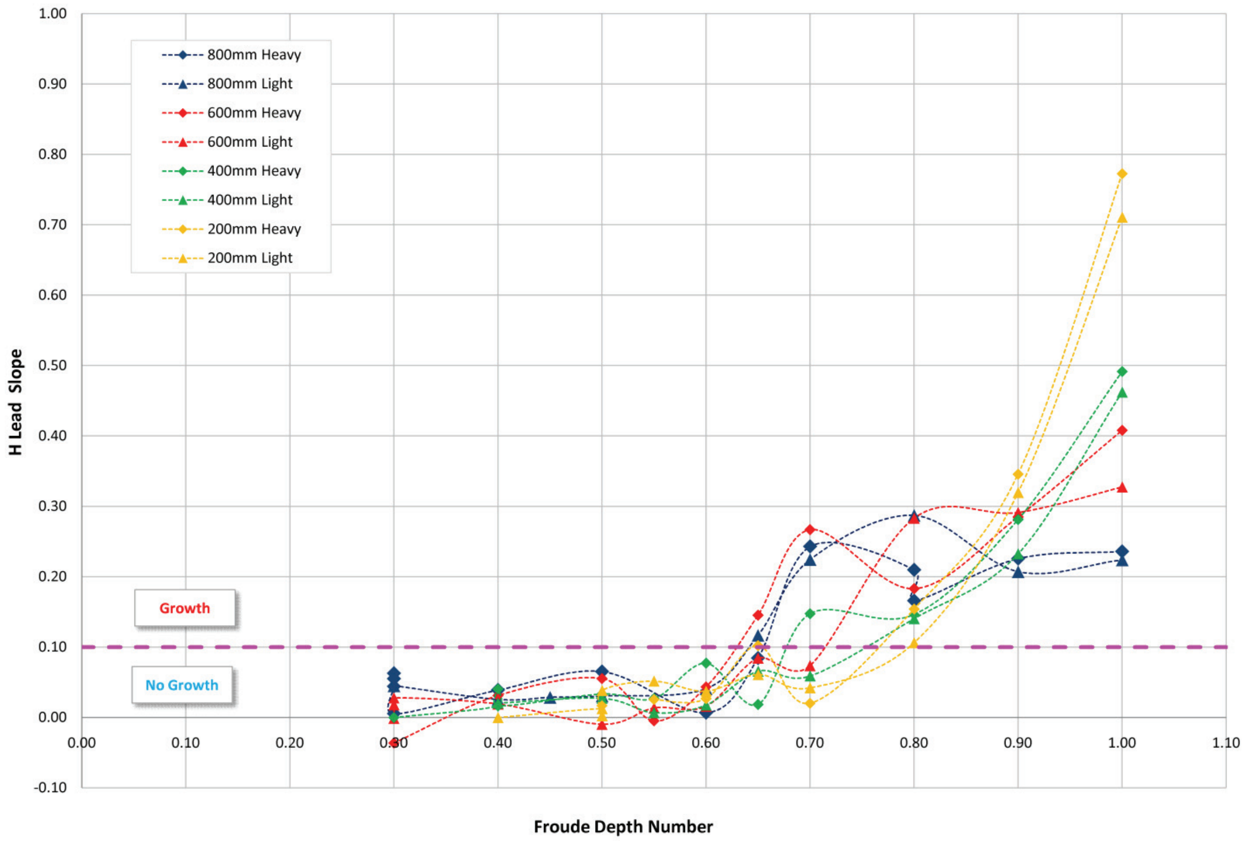

Figure 9 – Leading Wave Slope

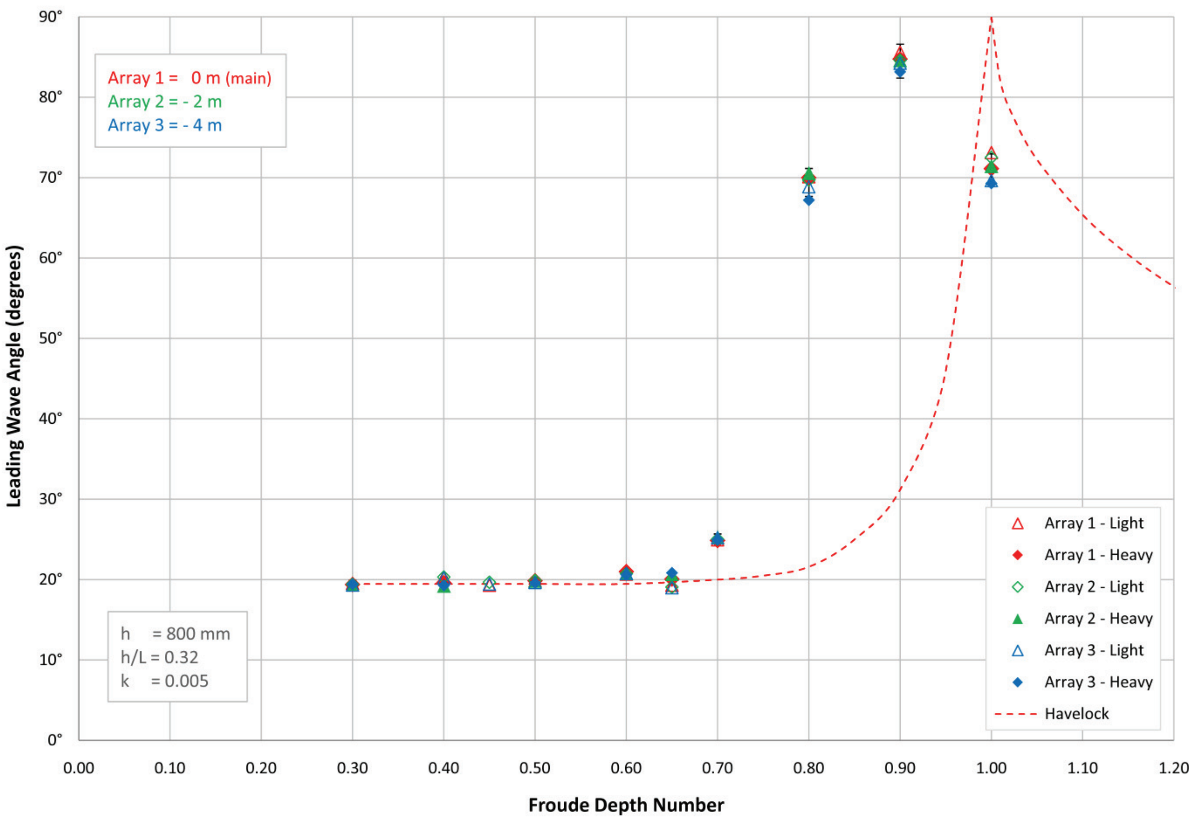

Figure 10 - Leading Wave Angle (h = 800mm)

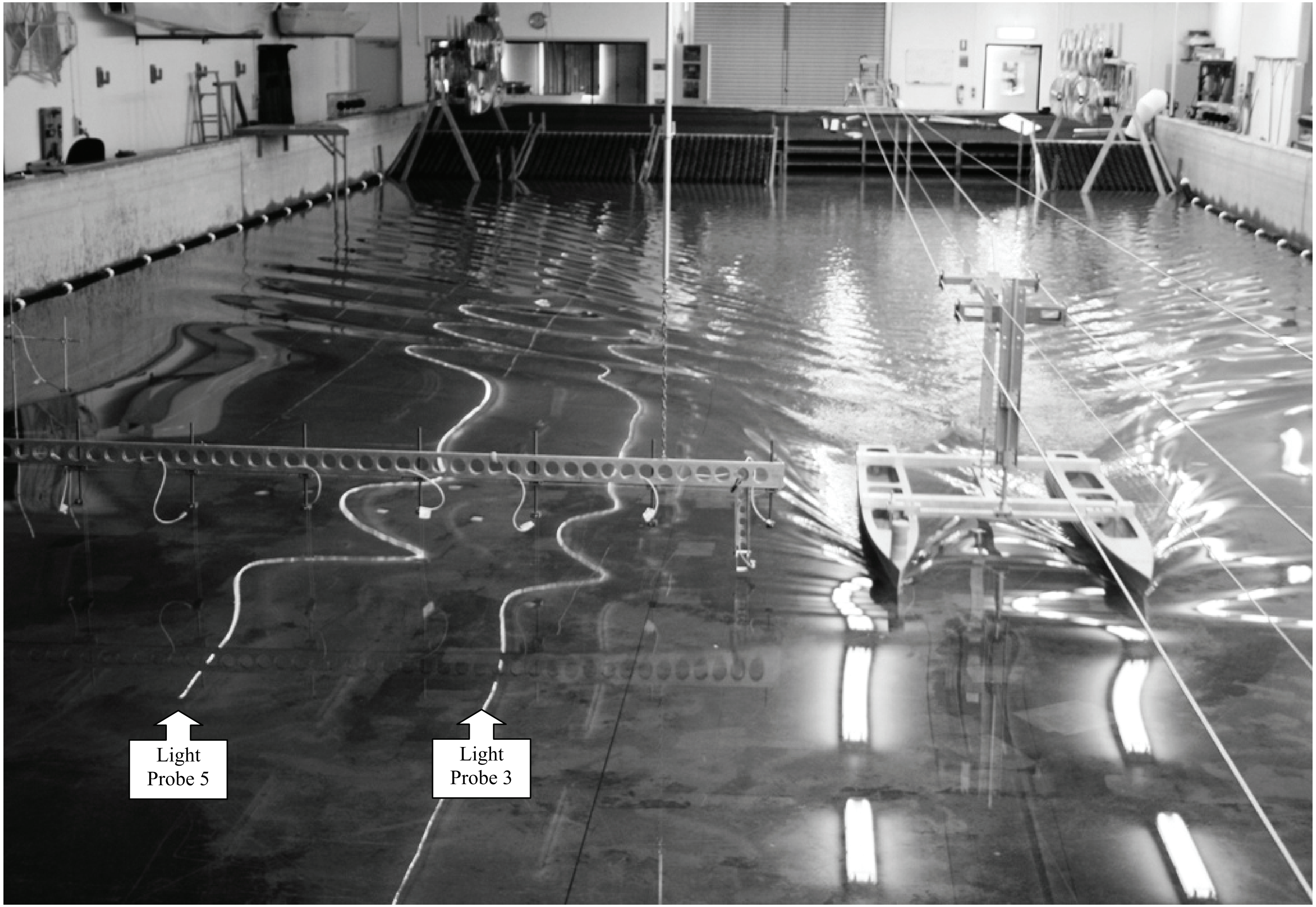

Figure 11 – $Fr_h = 1.0$, h = 200mm – Soliton

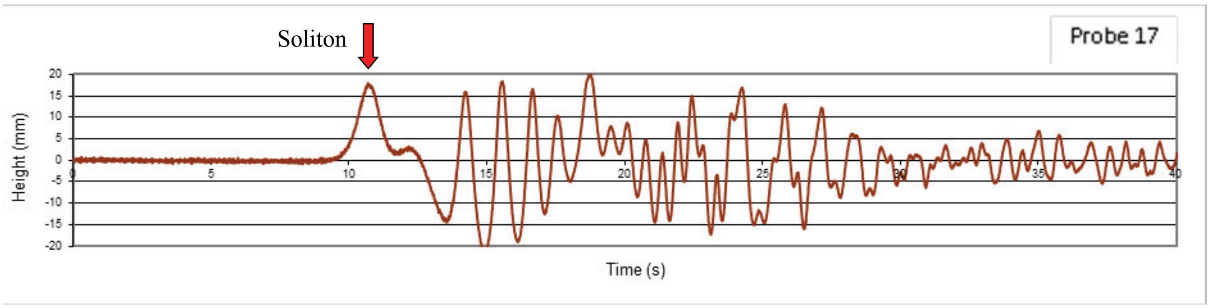

Figure 12 – Fr_h = 1.0, h = 200mm - Soliton

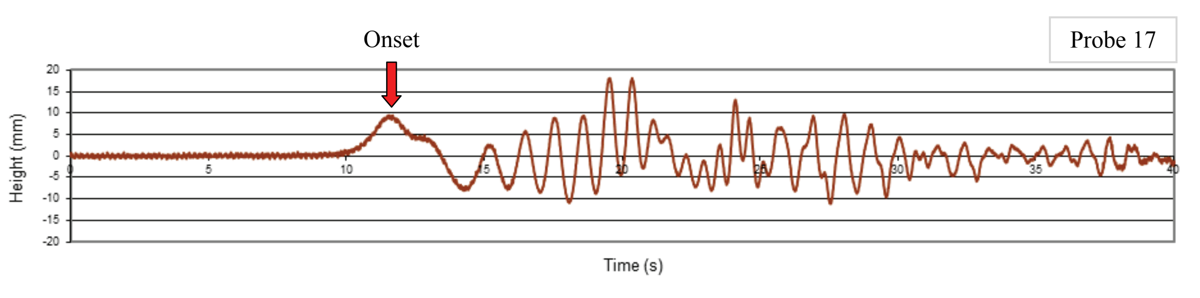

Figure 13 – Fr_h = 0.9, h = 200mm - Soliton Onset

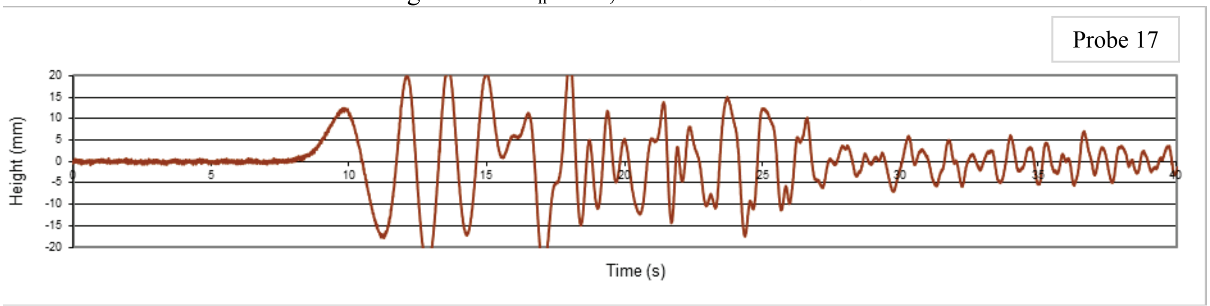

Figure 14 - Fr_h = 1.0, h = 400mm – No Soliton Detected

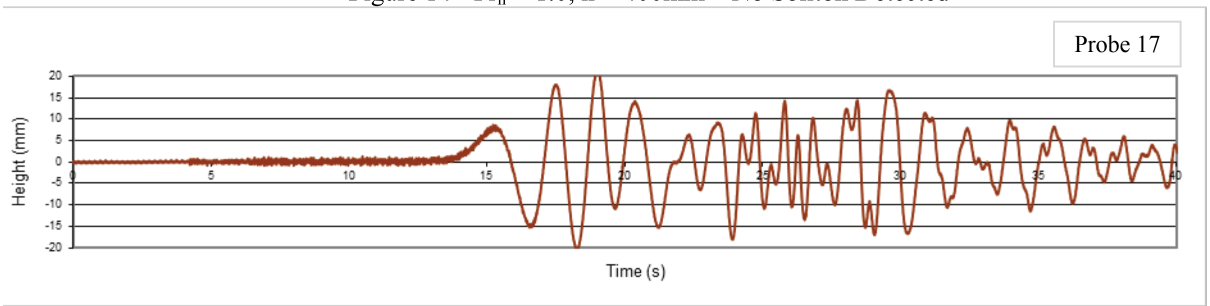

Figure 15 - Fr_h = 1.0, h = 600mm – No Soliton Detected

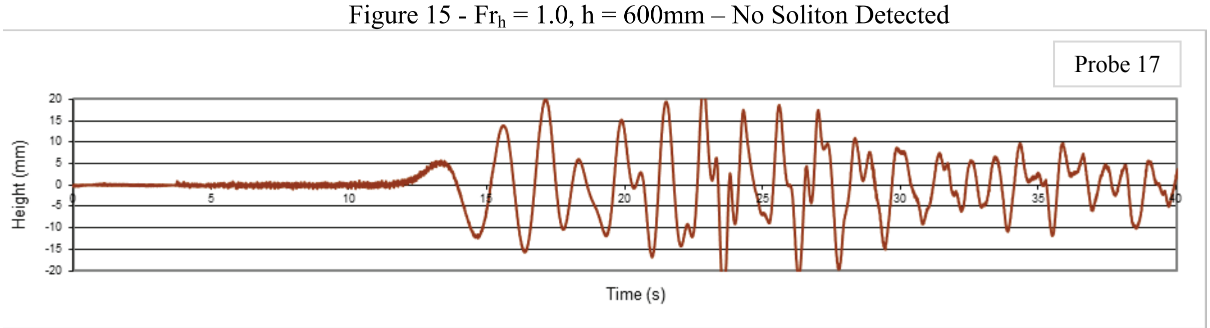

Figure 16 - Fr_h = 1.0, h = 800mm – No Soliton Detected

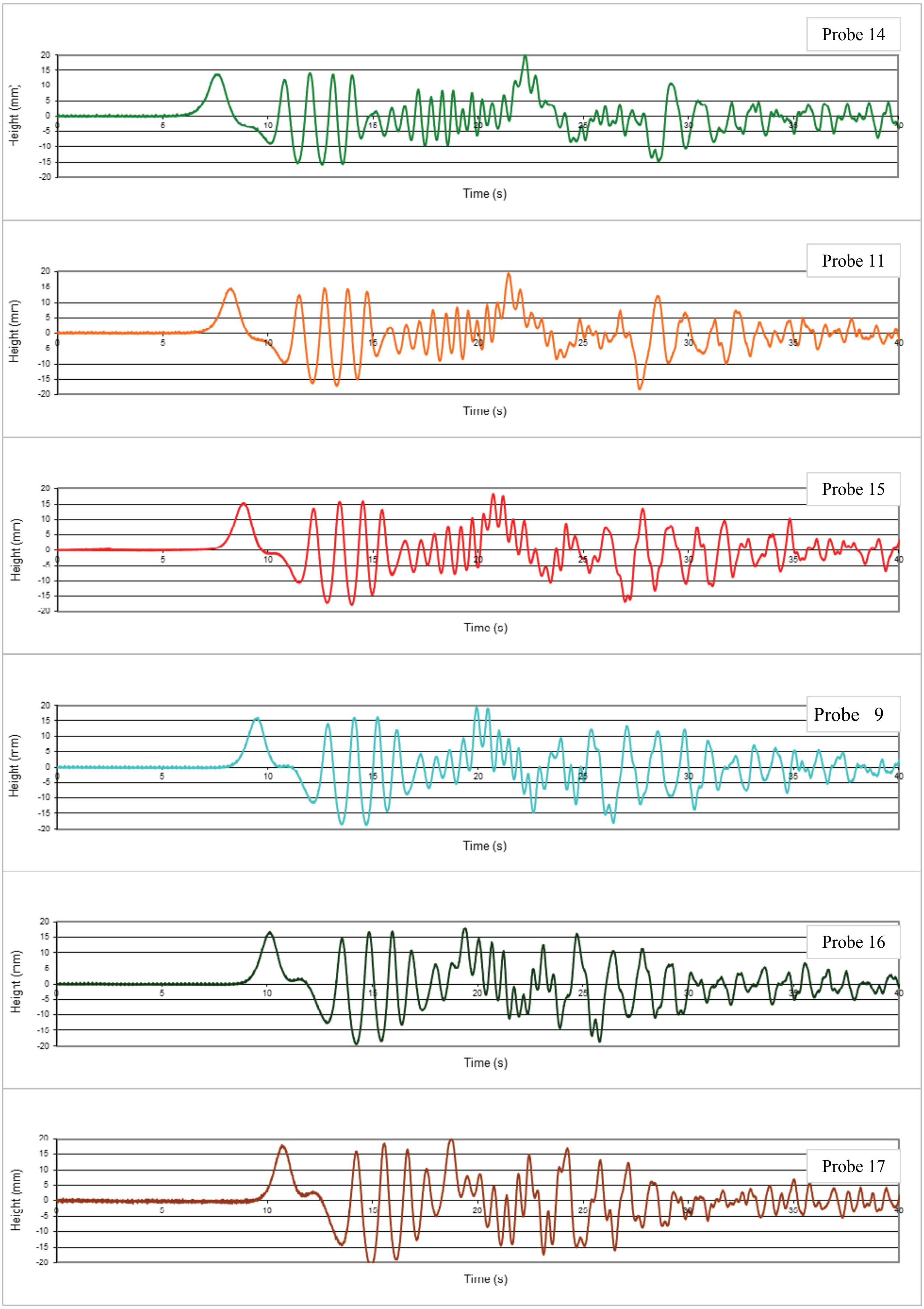

Figure 17 - Fr_h = 1.0, h = 200mm, Heavy – Soliton Development

Zone		Metric		
		Steadiness [1]	Bow Wave Angle [2]	Soliton [3]
1	Sub-Critical Deep	dy/dx < 0.1	$\theta_{bow} < 20°$	None
2	Sub-Critical Shallow	dy/dx > 0.1	$\theta_{bow} > 20°$	None
3	Critical Shallow	dy/dx > 0.1	$\theta_{bow} > 20°$	Observed
Steadiness [1]		= dy/dx < 0.1 (as per Figure 9)		
Bow Wave Angle [2]		= Deep = θ_{bow} < 20 ; Shallow = θ_{bow} >20		
Soliton [3]		= Soliton observed in longitudinal wave cut (@ probe 17)		

Table 3 – Proposed Shallow Water Metrics

Condition h / k		Depth Froude Number					
		0.5	0.6	0.7	0.8	0.9	1.0
Condition 8 h = 200mm k = 0.0141	Steadiness [1]	Steady	Steady	Steady	Unsteady	Unsteady	Unsteady
	Wave Angle [2]	Deep	Deep	Shallow	Shallow	Shallow	Shallow
	Soliton [3]	None	None	None	None	Onset	Soliton
	Zone [4]	1	1	2	2	2	3
Condition 5 h = 400mm k = 0.0070	Steadiness [1]	Steady	Steady	Unsteady	Unsteady	Unsteady	Unsteady
	Bow Wave [2]	Deep	Deep	Shallow	Shallow	Shallow	Shallow
	Soliton [3]	None	None	None	None	None	None*
	Zone [4]	1	1	2	2	2	2
Condition 4 h = 600mm k = 0.0047	Steadiness [1]	Steady	Steady	Unsteady	Unsteady	Unsteady	Unsteady
	Bow Wave [2]	Deep	Deep	Shallow	Shallow	Shallow	Shallow
	Soliton [3]	None	None	None	None	None	None*
	Zone [4]	1	1	2	2	2	2
Condition 1 h = 800mm k = 0.0035	Steadiness [1]	Steady	Steady	Unsteady	Unsteady	Unsteady	Unsteady
	Bow Wave [2]	Deep	Deep	Shallow	Shallow	Shallow	Shallow
	Soliton [3]	None	None	None	None	None	None*
	Zone [4]	1	1	2	2	2	2
Steadiness [1]	= dy/dx < 0.1 (as per Figure 9)						
Bow Wave Angle [2]	= Deep = θ_{bow} < 20 ; Shallow = θ_{bow} >20						
Soliton [3]	= Soliton observed in longitudinal wave cut (@ probe 17)						
None*	= No Solitons observed – (possibly due to limited run time)						
Zone [4]	= As specified in Table 3 above						

Table 4 – AMC MTB Results

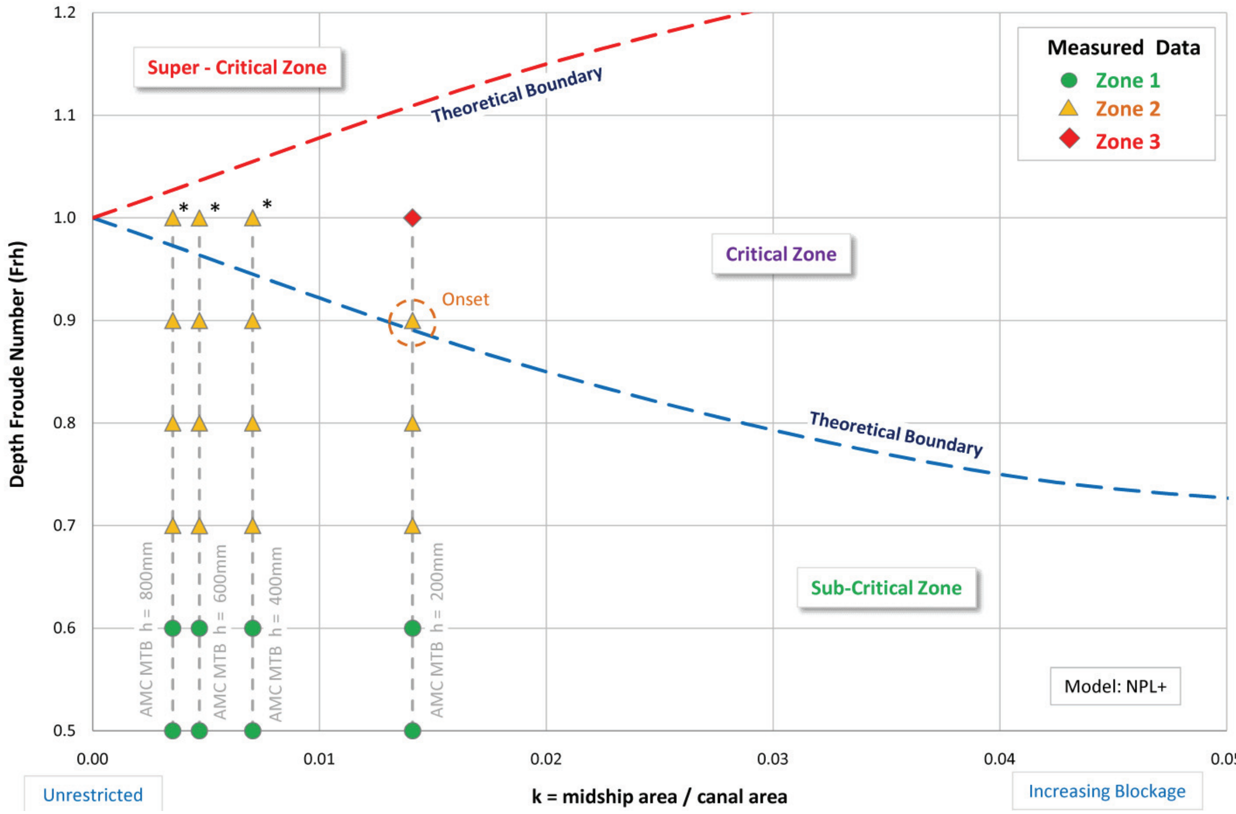

Figure 18 - Critical Boundaries with Measured Data Points